energies

MDPI

Article

Performance Evaluation of Air-Based Photovoltaic Thermal Collector Integrated with Dual Duct and Semicircular Turbulator in Actual Climate Conditions

Byeong-Hwa An [1], Seong-Bhin Kim [1], Hwi-Ung Choi [2] and Kwang-Hwan Choi [3,*]

[1] Graduate School of Refrigeration and Air-Conditioning Engineering, Pukyong National University, Busan 48513, Republic of Korea; or7i16@naver.com (B.-H.A.); tjdqls3821@naver.com (S.-B.K.)
[2] Department of Refrigeration and Air-Conditioning Engineering, Chonnam National University, Yeosu 59626, Republic of Korea; choihu@jnu.ac.kr
[3] Department of Refrigeration and Air-Conditioning Engineering, Pukyong National University, Busan 48513, Republic of Korea
* Correspondence: choikh@pknu.ac.kr

Abstract: An air-based photovoltaic thermal collector (PVTC) is a system that generates both electricity and heat using air flowing over a photovoltaic (PV) module. This system offers the advantage of easy maintenance; however, it suffers from lower thermal efficiency compared to other PVTCs, mostly owing to the low heat capacity of air. Thus, this study introduces a novel PVTC incorporating dual ducts and semicircular turbulators, which were experimentally evaluated under actual weather conditions in the Republic of Korea. The proposed PVTC was compared with two other types of PVTC: one is a single-duct PVTC with semicircular turbulators, and the other is a dual-duct PVTC without turbulators. The results showed that the thermal efficiency of the proposed PVTC increased by approximately 88.7% compared to the single-duct PVTC with a turbulator and by 9.3% compared to the dual-duct PVTC without a turbulator. The electrical efficiency showed a slight decrease of about 7.2% compared to the single-duct PVTC but an increase of 1.4% compared to the dual-duct PVTC without a turbulator. Overall, the total efficiency of the proposed PVTC increased by 54.2% and 7.7% compared to the single-duct PVTC and the dual-duct PVTC without a turbulator, respectively. These experimental results demonstrate that attaching dual ducts and semicircular turbulators to an existing PVTC increases the daily thermal energy output, which ultimately enhances the total daily energy output.

Keywords: solar energy; photovoltaic thermal collector; experiment; dual duct; turbulator

Citation: An, B.-H.; Kim, S.-B.; Choi, H.-U.; Choi, K.-H. Performance Evaluation of Air-Based Photovoltaic Thermal Collector Integrated with Dual Duct and Semicircular Turbulator in Actual Climate Conditions. *Energies* **2024**, *17*, 2752. https://doi.org/10.3390/en17112752

Academic Editors: Mario Petrollese, Marco Francesconi and Elisa Sani

Received: 30 April 2024
Revised: 29 May 2024
Accepted: 3 June 2024
Published: 4 June 2024

1. Introduction

As climate change and industrial development have driven a surge in energy demand, the importance of energy has been increasingly recognized. The use of renewable energy systems has expanded significantly to address these issues. Among them, photovoltaic (PV) systems, which are easy to install and have simple structures, are the most widely used. However, PV systems have a low solar energy conversion efficiency of approximately 10–20% and suffer from a decrease in power generation efficiency as the temperature of the solar cells increases [1,2].

To address these issues, Wolf [3] first proposed the concept of a photovoltaic thermal collector (PVTC). The PVTC cools the surface of the PV modules by circulating a fluid, thereby preventing a reduction in the power output due to overheating of the PV module. In addition, the heat recovered through this fluid can be utilized as another heat source. Among the various types of PVTCs, air-based PVTCs are preferred because of their low cost and easy maintenance, although they have a lower thermal efficiency than the others. Therefore, several studies have been conducted on enhancing the performance of air- based

PVTCs. One method involves installing structures such as ribs, baffles, or turbulators on the rear of the PV module to promote turbulence, thereby enhancing the overall efficiency.

Yadav and Bhagoria investigated a two-dimensional computational fluid dynamics (CFD) model for PVTCs that incorporated equilateral triangular [4] and square [5] turbulators on an absorber plate. They analyzed the effects of the turbulator's variables such as the relative installation spacing, relative installation height, and coolant flow rate on heat transfer and friction. The thermo-hydraulic performance (THP) is significantly influenced by the relative installation height, and the friction factor increases with height. Kumar et al. [6] evaluated the THP by attaching multiple V-shaped perforated baffles to the air channels of PVTCs. In order to reduce the friction factor of the thermal fluid, the optimal shape of the baffle was proposed through CFD, and the heat transfer performance according to the flow rate was evaluated through actual experiments by applying circular holes to the baffle. Kumar et al. [7] conducted a CFD analysis on triangular PVTC air channels using forward-facing chamfered rectangular ribs and confirmed that these ribs enhanced both the heat transfer performance and friction factor. Recently, Kim et al. [8] assessed the pressure drop and heat transfer performance of turbulator shapes within PVTCs using CFD analysis. The performance was compared with triangular, square, and semicircular turbulator shapes with increasing turbulator ratios, and it was verified that, based on the THP, semicircular shapes provided the highest performance, followed by triangular and square shapes. Kim et al. [9] applied semicircular turbulators to a PVTC simulation model to evaluate its performance under various flow conditions and turbulator shape configurations. They presented correlation formulas related to the flow and geometrical conditions of semicircular turbulators. Additionally, various studies have shown that installing turbulators on a flat plate under constant heat flux conditions can enhance performance [10–13].

Based on the above studies, it was confirmed that installing structures such as turbulators can enhance the performance of PVTCs. Other methods to improve PVTC performance include changing the fluid flow or creating additional flow paths. Several researchers [14–16] have compared and evaluated the performance of dual-duct PVTCs, where air enters through an upper channel and exits through a lower channel. It was found that this dual-duct configuration performed better than single-duct PVTCs. Amori et al. [17] compared PVTCs in which air flows in the same direction through both the upper and lower channels with PVTCs in which air enters the upper channel and exits the lower channel. It was verified that the dual-flow-path PVTC with the same airflow direction performed better than the PVTC with opposite airflow. Hegazy [18] conducted a comparative study on the performance of flat-plate PVTCs for four different designs: air flowing over the absorber, under the absorber, on both sides of the absorber in a single pass, and in a double pass. The results indicated that the models with dual ducts exhibited better energy efficiency than those with single ducts. Hussain et al. [19] evaluated single- and dual-channel structures for air-based PVTCs and examined the performance differences between parallel- and counter-flow configurations within a dual channel. They compared different types of designs and described their performance characteristics. Ooshaksaraei et al. [20] conducted indoor experiments using a solar simulator to compare the energy and exergy efficiencies of four PVTC designs. Their findings showed that the dual-channel parallel flow model exhibited the highest energy efficiency, ranging between 51% and 67%, whereas the single-channel path model displayed the best exergy efficiency, with values ranging between 8.2% and 8.4%. These results confirm that if the goal is to maximize the thermal energy output, dual-channel designs are advantageous, whereas single-channel designs are more appropriate when the main objective is electrical output. Additionally, various studies have been conducted to explore the enhancement of heat transfer performance in PVTCs by modifying the fluid flow paths [21].

The studies reviewed above improved the heat transfer performance of PVTCs by either attaching turbulators or changing the airflow path. Nevertheless, there has been very limited research that simultaneously considers both factors. Othman et al. [22] experi-

mentally assessed the electrical and thermal performance of PVTCs with dual air channels and fins attached to the back of an absorber plate. They confirmed that the addition of fins to the dual-duct PVTC improved the overall efficiency. Choi et al. [23] experimentally evaluated the performance of a single-pass double-flow PVTC with non-uniform cross-sectional transverse ribs under actual meteorological conditions by varying the air mass flow rate. Alam et al. [24] conducted numerical analyses to determine the optimal shape for the protrusion of triangular ribs and applied this ribbed design to a dual-duct PVTC for performance evaluation. However, studies that simultaneously apply dual ducts and turbulators are rare, and the shapes of these turbulators are limited to triangular forms. This gap in the literature motivates the current research.

Therefore, this study proposes an air-based PVTC that is integrated with a semicircular turbulator and a dual duct, which was experimentally evaluated. The collector featured a semicircular turbulator installed at the back of the PV module, and glass was placed over the PV module to form a dual duct. The main objective of this study was to verify the performance of the proposed PVTC by specifically assessing the effects of dual ducts and turbulators. Therefore, to confirm the performance enhancement of the proposed design, two other types of PVTCs were evaluated under the same conditions: a single-duct PVTC equipped with semicircular turbulators and a dual-duct PVTC without turbulators. This study provides fundamental data for improving PVTCs' performance and can serve as crucial information to enhance solar energy conversion efficiency in the future.

2. Experimental Setup and Procedure

2.1. Description of Air-Based PVTC

Figure 1 shows a schematic of a dual-duct PVTC that was integrated with a semicircular turbulator. The air-based PVTC consisted of a commercial photovoltaic module, a lower air channel equipped with semicircular turbulators, and an upper channel made of glass. Semicircular turbulators were attached to the back of the PV module. The PV system used was a commercial product (LG electronics Inc., LG450S2W-U6, Republic of Korea), and its characteristics are listed in Table 1.

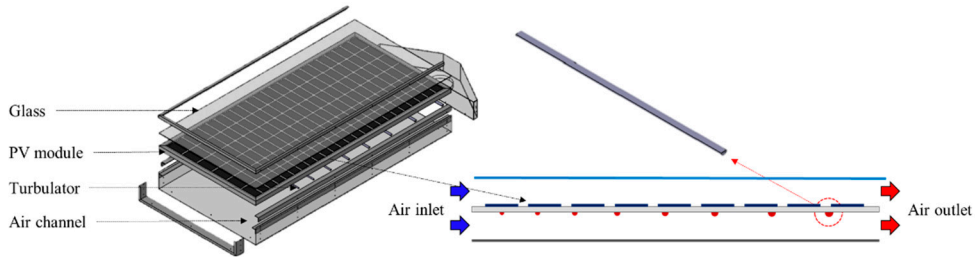

Figure 1. Schematic of dual-duct PVTC integrated with semicircular turbulator.

Table 1. Characteristics of the PV module under standard conditions.

Parameters	Value
Size of module (mm)	2011 × 1042 × 40
Electrical efficiency (%)	20.2
Temperature coefficient (%/°C)	−0.27
Maximum output power (W)	450
Output voltage at maximum power (V)	40.91
Output current at maximum power (A)	11.01

Figure 2 shows a schematic of the two-dimensional dual-duct PVTC coupled with semicircular turbulators. The total width, length, and height of the proposed PVTC were 1042 mm, 2017 mm, and 200 mm, respectively. The lower and upper air channels have a height (h) of 80 mm.

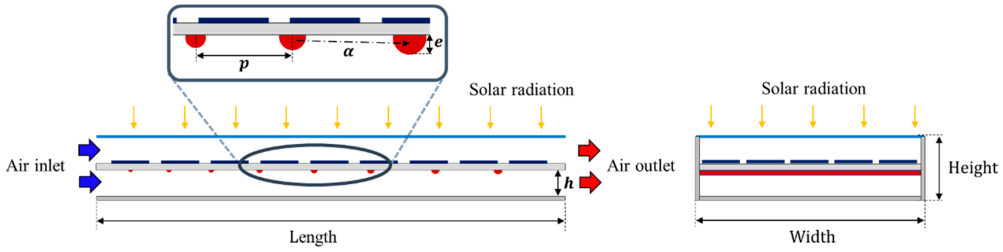

(**a**) Side view (**b**) Front view

Figure 2. Schematic of two-dimensional dual-duct PVTC coupled with semicircular turbulator.

The turbulators were designed with a semicircular shape, and parameters such as height (e), pitch (p), and increase ratio (α) were specified based on definitions established in previous studies [11]. The increase ratio (α), representing the rise in height (e) and pitch (p) of the turbulators installed in the previous array, enhanced the heat transfer performance while reducing the pressure drop. To make the shape conditions of the turbulators dimensionless, the relative height (e/h) and relative pitch (p/e) were used. Table 2 summarizes the geometric conditions of the PVTC and semicircular turbulator.

Table 2. Geometric conditions of PVTC and semicircular turbulator.

Parameters		Value
PVTC	Width (mm)	1042
	Length (mm)	2017
	Height (mm)	200
	Upper- and lower channel height (h) (mm)	80
Semicircular turbulator	α (-)	1.11
	e/h (-)	0.116
	p/e (-)	17.94

In addition, two other types of PVTCs were fabricated to verify the performance improvement of the proposed PVTC: a single-duct PVTC with semicircular turbulators (Type A) and a dual-duct PVTC without any turbulence (Type B). Figure 3 shows schematic side views of the three different types of PVTCs. The single-duct PVTC with semicircular turbulators, designated as Type A, featured a semicircular turbulator attached to the rear of the PV module. Additionally, the dual-duct PVTC without any modifications, known as Type B, incorporated glass positioned above the PV module to create an upper air channel. The dual-duct PVTC with semicircular turbulators, referred to as Type C, combined a dual-duct design with semicircular turbulators, as proposed in this study.

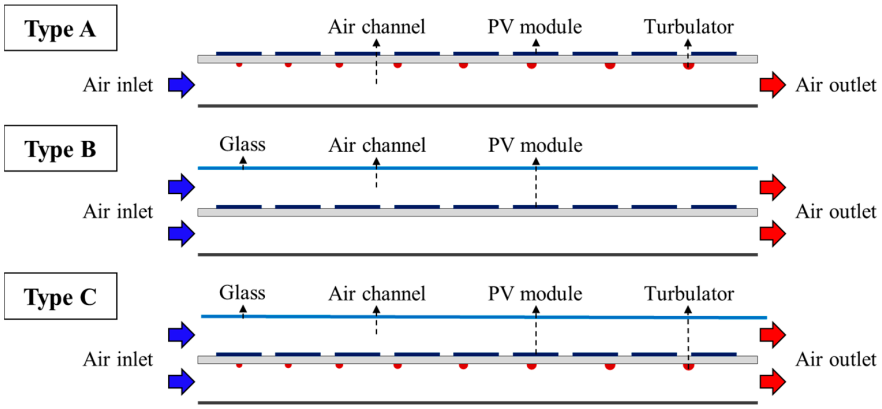

Figure 3. Schematic side view of three different types of PVTCs.

2.2. Experimental Procedure

Figure 4 shows an actual view of the experimental apparatus. The experiments were conducted under actual weather conditions on the same day for the PV and the three different types of PVTCs. The experimental setup was located at the Pukyong National University's Yongdang Campus in Busan, Republic of Korea (latitude: 35°6.98′, longitude: 129°5.39′). The installation angle was 21°. Each PVTC maintained a constant airflow rate of 0.077 kg/s using ambient air as the inlet. The experiments were conducted from 10:30 a.m. to 2:30 p.m. on 12 April 2023.

Figure 4. Actual view of experimental setup.

Figure 5 illustrates the schematic of the experimental setup and the measuring device locations. The experimental system included the PVTC, along with a fan (INNOTECH Corporation, TIS-140FS, Japan) and a battery (Hankook AtlasBX Co., Ltd., SB1000, Republic of Korea) to facilitate air flow within the PVTC. The fan provided an air flow rate of 0.077 kg/s, and the battery had a capacity of 1 kW. The data collected included solar irradiance, as well as current and voltage generated by the PV, ambient temperature, PV surface temperature, and outlet air temperature from the PVTC. The voltage and current were measured with a voltmeter (Autonics Corporation Co., Ltd., MT4Y-DV-43, Republic of Korea) and an ampere meter (Autonics Corporation Co., Ltd., MT4Y-DA-43, Republic of Korea), respectively. The solar radiation was measured with a pyranometer (EKO Instruments Co. Ltd., MS-802, Japan), while air temperatures were measured with T-type thermocouples. Additionally, an anemometer (Kanomax Japan Inc., 6531-2G, Japan) was used to measure air velocity. The detailed specifications of each measurement are listed in Table 3.

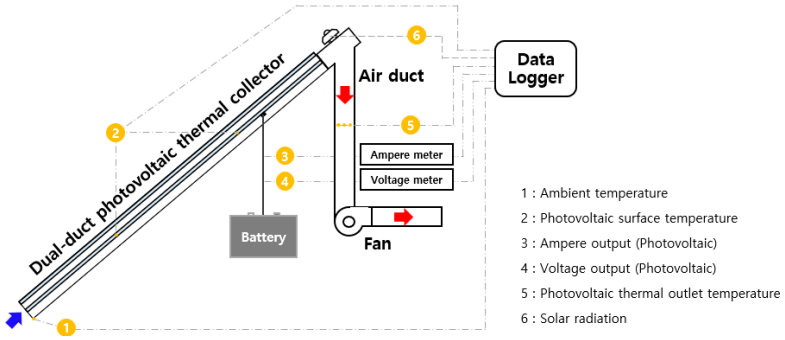

Figure 5. Schematic of the experimental setup and the measuring device locations.

Table 3. Specifications of measuring devices.

Device	Model	Range	Uncertainty
Pyranometer	MS-802	0–4000 W/m^2	±2%
Voltmeter	MT4Y-DV-43	0–50 V	±0.56%
Ampere meter	MT4Y-DA-43	0–5 A	±0.56%
Thermocouple	T-type	−281–370 °C	±1 °C
Anemometer	Kanomax 6531-2G	0.01–9.99 m/s	±2%
Data logger	Agilent 34972A	-	-

2.3. Uncertainty Analysis

In the experimental data related to the PVTC, errors may appear due to a sensor measuring various elements and introducing uncertainties. Thus, to accurately evaluate the primary performance of the PVTC, assessing the error associated with each performance value is necessary [25]. The uncertainty of a parameter is obtained as follows:

$$\mathrm{y} = \mathrm{f}(x_1, x_2, \cdots, x_n). \tag{1}$$

$$\delta y = \sqrt{\left(\frac{\delta y}{\delta x_1}\delta x_1\right)^2 + \left(\frac{\delta y}{\delta x_2}\delta x_2\right)^2 + \cdots + \left(\frac{\delta y}{\delta x_n}\delta x_n\right)^2}, \tag{2}$$

where δx_1,δx_2, $\cdots$, δx_n represent the uncertainties in the directly measured values. The main factors of the PVTC's performance assessed in this research are Q_{air}, η_{th}, W_{pv}, η_{el}, and η_o. The uncertainties and parameters are detailed in Table 4.

Table 4. Parameter uncertainties for each experimental setup.

Parameter	Uncertainty
Q_{air}	±2.26%
η_{th}	±3.02%
W_{pv}	±0.97%
η_{el}	±2.22%
η_o	±3.17%

2.4. Performance Index

To evaluate the performance of the PVTC, the main factors considered were power generation, electrical efficiency, heat gain, thermal efficiency, and total efficiency [17]. The electricity generation of the PV system (W_{pv}) can be calculated using Equation (3).

$$\mathrm{W}_{pv} = V_{pv} I_{pv}, \tag{3}$$

where V_{pv} and I_{pv} are the voltage and current produced by the PV module, respectively. The electrical efficiency of the PVTC (η_{el}) can be obtained using Equation (4).

$$\eta_{el} = \frac{W_{pv}}{G A_{PVTC}}, \tag{4}$$

where G is the solar radiation, and A_c is the area of the PVTC. The heat gain (Q_{air}) of the PVTC can be calculated using Equation (5).

$$Q_{air} = \dot{m}_{air} C_{p,air} (T_{air,out} - T_{air,in}), \tag{5}$$

where $\dot{m}_{air}$, $C_{p,air}$, T_{airout}, and T_{airin} denote the mass flow rate of air, specific heat of air, outlet air temperature, and inlet air temperature, respectively. The thermal efficiency (η_{th})

of a PVTC is the ratio of incoming solar radiation and heat gain of the PVTC and can be obtained using Equation (6).

$$\eta_{th} = \frac{Q_{air}}{GA_{PVTC}}. \quad (6)$$

The overall efficiency (η_o) of a PVTC is calculated using Equation (7):

$$\eta_o = \eta_{el} + \eta_{th}. \quad (7)$$

3. Results and Discussion

3.1. Weather Conditions

Figure 6 shows the ambient temperature and solar radiation during the test period. The ambient temperature ranged from 15.32 °C to 17.64 °C, and the solar radiation varied between 915.15 W/m^2 and 1017.70 W/m^2. The average ambient temperature was 16.45 °C, and the average solar radiation was 993.50 W/m^2 during the test period. Peak solar radiation was observed at 12:20 p.m. local time, and the highest ambient temperature was recorded at 1:00 p.m. local time in the Republic of Korea. The graph also indicates that the experiment was carried out on a clear day, which is ideal for assessing the performance of PVTCs under optimal sunlight conditions.

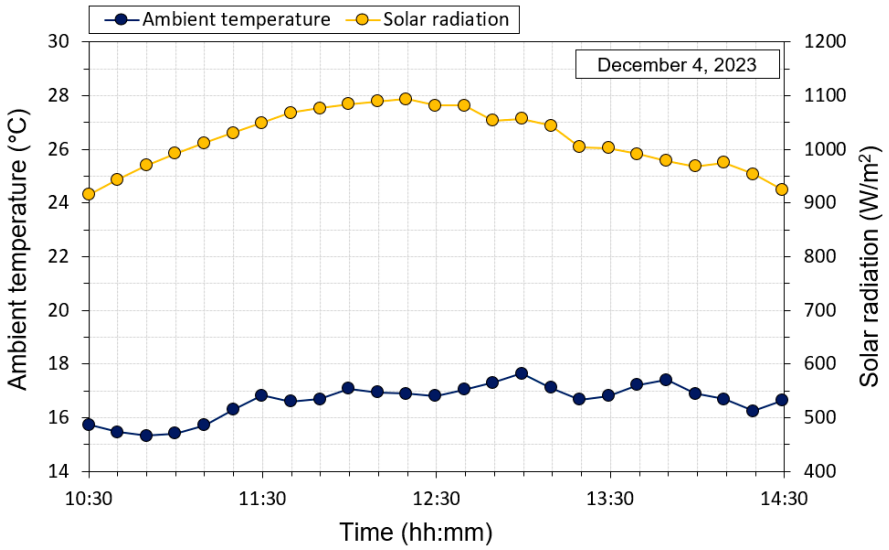

Figure 6. Ambient temperature and solar radiation during test period.

3.2. Thermal Performance

Figure 7 shows the air temperature increase for the different types of PVTCs. The air temperature increased from 4.90 °C to 6.50 °C, 8.59 °C to 11.11 °C, and 9.25 °C to 12.23 °C for Type A, Type B, and Type C, respectively. The average air temperature increase during the experiment period was 5.76 °C, 9.94 °C, and 10.87 °C for Type A, Type B, and Type C, respectively. These results show that Type C, featuring semicircular turbulators, experienced an average air temperature increase of 0.92 °C compared to Type B, which does not have semicircular turbulators. In addition, it was observed that Type C, equipped with a dual duct, showed an increase of 5.11 °C in temperature compared to Type A, which features a single duct. The outlet air temperature increased with increasing solar radiation and then decreased with decreasing solar radiation. Throughout this period, Type C consistently maintained a higher outlet temperature than the other types. This confirms that PVTCs equipped with semicircular turbulators and dual ducts offer enhanced heat transfer performance in the air flow channel compared with other types of PVTCs.

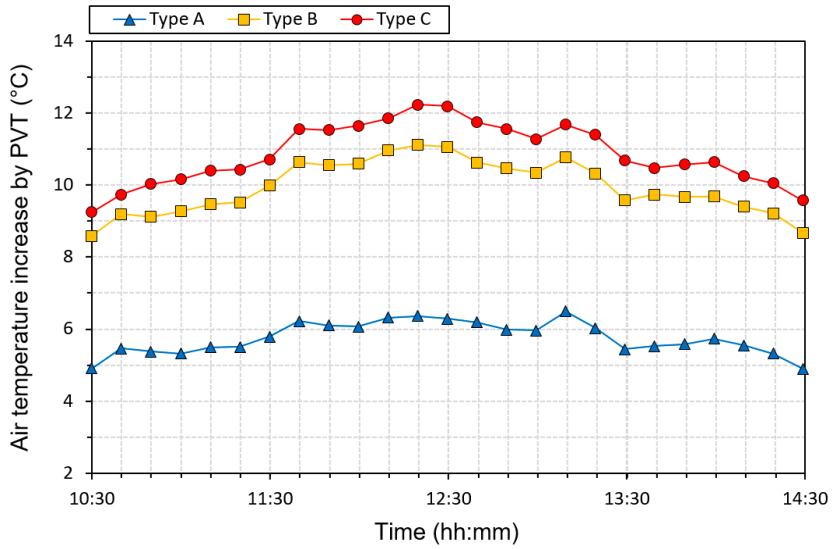

Figure 7. Air temperature increase for different types of PVTCs.

Figure 8 illustrates the PV surface temperatures for different types of PVTCs. The solar cell temperature ranged from 41.1 °C to 48.1 °C, 32.0 °C to 38.6 °C, 60.5 °C to 70.6 °C, and 52.7 to 61.6 °C for PV, Type A, Type B, and Type C, respectively. The average solar cell surface temperature was 44.8 °C, 35.7 °C, 66.8 °C, and 57.9 °C for PV, Type A, Type B, and Type C, respectively. Throughout the experimental period, Type B consistently exhibited the highest surface temperature, whereas Type A consistently exhibited the lowest. The PV surface temperature increased with increasing solar radiation and then decreased with decreasing solar radiation. In addition, Type A had a lower surface temperature than PV, because the forced convection of air by the fan removed more heat from the PV module. In the case of Type C, which includes turbulators, these devices promote air turbulence, leading to lower temperatures compared with Type B, which does not include turbulators. Furthermore, both Type B and Type C, which utilize a dual-duct system, exhibited higher temperatures than the other types. This is because the glass prevents the heat generated by the PV module from radiating to the outside air.

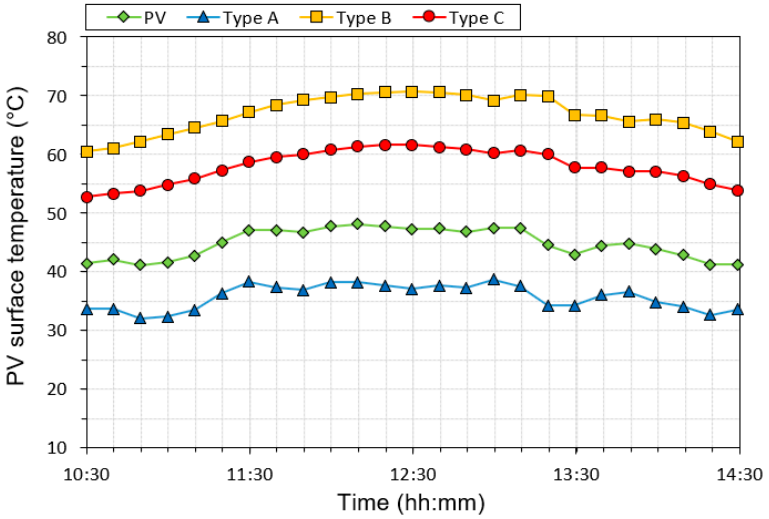

Figure 8. PV surface temperature for different types of PVTCs.

Figure 9 shows the heat gain and thermal efficiency for the different types of PVTCs. The heat gains of Type A, Type B, and Type C ranged from 378.8 W to 502.1 W, 663.6 W to 858.9 W, and 714.8 W to 945.1 W, respectively. The average heat gains for Type A,

Type B, and Type C were 445.0 W, 768.4 W, and 839.7 W, respectively. The thermal efficiencies of Type A, Type B, and Type C ranged from 20.5% to 24.1%, 35.7% to 39.9%, and 39.1% to 43.9%, respectively. The average thermal efficiencies of Type A, Type B, and Type C were 21.9%, 37.7%, and 41.2%, respectively. It was confirmed that the average thermal efficiency of Type C was improved by 88.1% and 9.3% compared with Type A and Type B, respectively. The above results confirmed that the average heat gain and thermal efficiency of Type C were higher than those of Type A and Type B. It was confirmed that in the dual-duct structure, most of the heat lost upward was not dissipated outside because of the glass, leading to an increase in thermal efficiency. In addition, the installation of turbulators enhanced the turbulence in the air channels, which enhanced the efficiency of the heat transfer between the heated surfaces of the PV module and the blowing air.

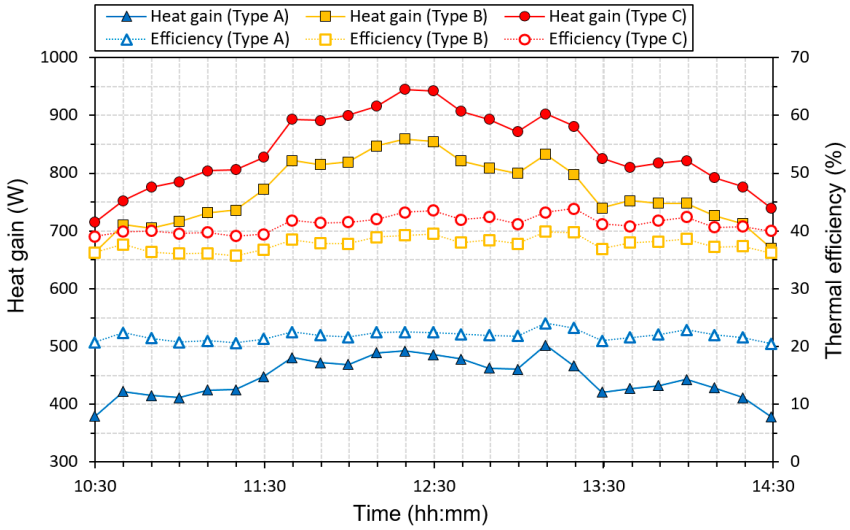

Figure 9. Heat gain and thermal efficiency for different types of PVTCs.

3.3. Electrical Performance

Figure 10 shows the power generation and electrical efficiency of the different types of PVTCs. The power generation of PV, Type A, Type B, and Type C were in the range of 245.9 W to 248.5 W, 252.5 W to 255.3 W, 227.1 W to 238.3 W, and 234.9 W to 241.4 W, respectively. The average power generation for each type was 247.3 W, 253.5 W, 231.9 W, and 236.8 W, respectively. The power generation efficiencies of PV and Type A, Type B, and Type C ranged from 13.4% to 16.1%, 13.7% to 16.5%, 12.6% to 15.4%, and 12.7% to 15.5%, respectively. The average electrical efficiencies of PV, Type A, Type B, and Type C were 14.5%, 14.8%, 13.6%, and 13.8%, respectively. Type A, with a single duct, exhibited the highest efficiency, with average increases of 2.07%, 8.82%, and 7.2% over PV, Type B, and Type C, respectively. The electrical performance of the PVTC was closely related to the PV surface temperature, as shown in Figure 8. It was observed that a decrease in the PV module's surface temperature owing to air cooling within the PVTC occurred in Type A. Type B and Type C exhibited a lower electrical efficiency than Type A, which was attributed to the dual-duct structure preventing heat from escaping through the glass above the PV module. Additionally, when a dual-duct structure is used, the addition of glass introduces its own reflectivity and absorptivity, which reduces the incoming solar radiation to the PV module in the PVTC. Consequently, both the power generation and the electrical efficiency of dual-duct PVTCs decrease. Furthermore, Type C demonstrated a higher efficiency than Type B did. This was attributed to the installation of turbulence promoters in the air channels, which enhanced the air turbulence and reduced the PV surface temperature, thereby increasing the generation efficiency.

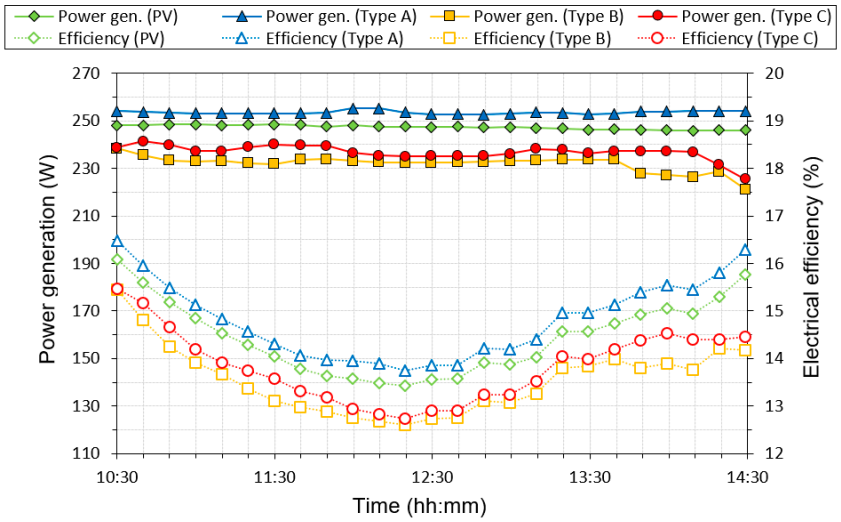

Figure 10. Power generation and electrical efficiency for different types of PVTCs.

3.4. Overall Efficiency

Figure 11 shows the overall efficiency of different types of PVTCs. The overall efficiency is the sum of thermal and power generation efficiencies. The overall efficiencies of Type A, Type B, and Type C ranged from 32.9% to 36.2%, 46.9% to 51.4%, and 50.6% to 55.7%, respectively. The average overall efficiencies of the PVTCs were 34.3%, 49.1%, and 52.9% for Type A, Type B, and Type C, respectively. The average overall efficiency of Type C was improved by 54.23% compared to that of Type A using a dual duct. In addition, the average overall efficiency of Type C was improved by 7.74% compared to that of Type B by using semicircular turbulators.

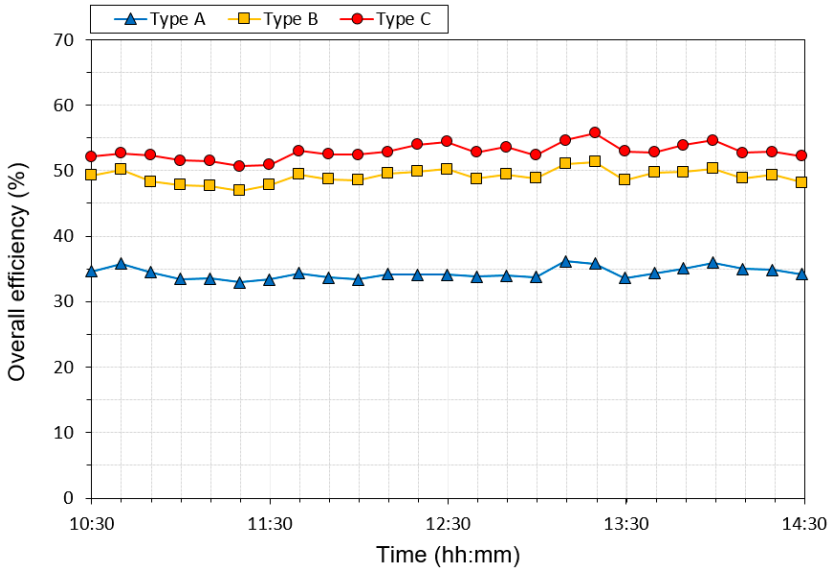

Figure 11. Overall efficiency for different types of PVTCs.

3.5. Total Energy Output

Figure 12 shows the total energy outputs of the different types of PVTCs during the experiment. The electrical outputs of Type A, Type B, and Type C were 528.2 Wh/m^2, 483.3 Wh/m^2, and 493.3 Wh/m^2, respectively, and the thermal outputs were 927.2 Wh/m^2, 1600.7 Wh/m^2, and 1749.3 Wh/m^2, respectively. The total daily energy outputs were 1455.4 Wh/m^2, 2084.0 Wh/m^2, and 2242.6 Wh/m^2, respectively. Type C had a 54.1% increase in the total daily energy output compared to Type A owing to the effect of the

dual ducts. In addition, the total daily energy output of Type C was 7.61% higher than that of Type B owing to the semicircular turbulator. As a result, the dual duct produced 88.7% additional thermal energy, with a 6.60% decrease in the electrical output, whereas the semicircular turbulator increased the electrical output by 2.07% and thermal output by 9.28%. Based on this, it was found that the installation of dual ducts and semicircular turbulators increased the total daily energy output compared with the conventional single-duct PVTC.

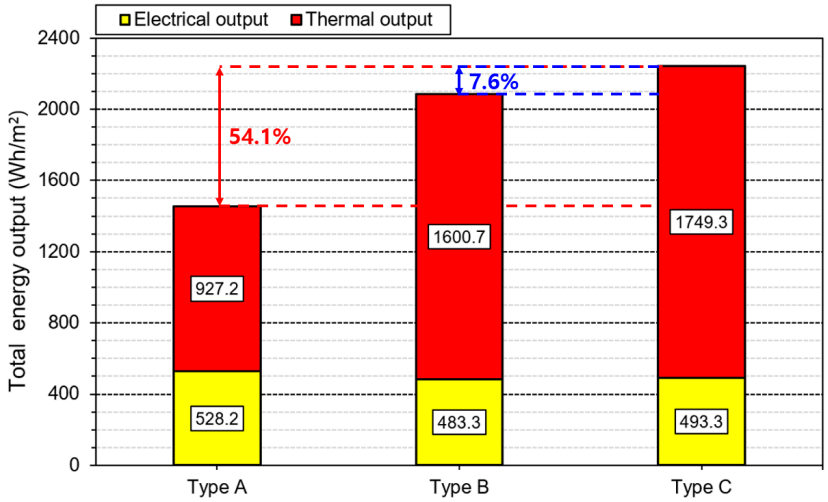

Figure 12. Total energy output for different types of PVTCs.

4. Conclusions

In this study, a dual-duct PVTC with semicircular turbulators (Type C) was evaluated experimentally and compared with a single-duct PVTC with semicircular turbulators (Type A) and a dual-duct PVTC without turbulators (Type B). The following conclusions can be drawn from the results:

(1) The average inlet and outlet air temperature difference was highest for Type C at 10.87 °C, compared to Type A at 5.76 °C and Type B at 9.94 °C. The average PV surface temperature was lowest in Type A at 35.7 °C, whereas for PV, Type B, and Type C, they were lowest at 44.8 °C, 66.8 °C, and 57.9 °C, respectively.

(2) Among the PVTCs, Type C with semicircular turbulators and dual-duct structures exhibited significant improvements in both thermal and electrical efficiency. The thermal efficiency of Type C increased by 9.3% compared to Type B and by 88.1% compared to Type A due to the installation of semicircular turbulators and the dual-duct structure. However, the electrical efficiency of Type C showed a decrease of 4.83% compared to Type A but increased by 1.47% compared to Type B.

(3) The average overall efficiencies were 34.3%, 49.1%, and 52.9% for Type A, Type B, and Type C, respectively. Type C exhibited a 54.23% increase in average overall efficiency compared to Type A, which utilized a single duct, and a 7.74% increase compared to Type B, which lacked semicircular turbulators.

(4) The electrical output of Type C was 6.60% lower than that of Type A; however, it was 2.07% higher than that of Type B. Additionally, the thermal output of Type C was 88.7% higher than that of Type A and 9.28% higher than that of Type B. Consequently, the total energy output of Type C was 54.1% higher than that of Type A and 7.61% higher than that of Type B.

This study confirmed that the simultaneous application of dual ducts and semicircular turbulators to PVTCs significantly increased both the thermal and overall efficiencies. Based on these results, we can provide foundational data for enhancing PVTC performance. The primary objective of creating such high-efficiency PVTCs is to facilitate their use in various fields, such as hot water supply, space heating, and drying systems, to reduce

energy consumption and assess their economic benefits. Therefore, future research should focus on analyzing the energy savings and economic benefits of the proposed PVTCs.

Author Contributions: Conceptualization, B.-H.A.; Methodology, H.-U.C.; Formal analysis, H.-U.C.; Investigation, B.-H.A.; Data curation, B.-H.A. and S.-B.K.; Writing—original draft, S.-B.K.; Writing—review & editing, H.-U.C. and K.-H.C. All authors have read and agreed to the published version of the manuscript.

Funding: This research received no external funding.

Data Availability Statement: The original contributions presented in the study are included in the article, further inquiries can be directed to the corresponding author.

Conflicts of Interest: The authors declare no conflict of interest.

Nomenclature

Symbols	
A	Area (m^2)
C_p	Specific heat capacity (J/kg°C)
G	Solar radiation (W/m^2)
I	Ampere (A)
Q	Heat transfer rate (W)
T	Temperature (°C)
V	Voltage (V)
W	Power (W)
e	Height of semicircular turbulator (m)
h	Height of air channel (m)
p	Pitch of turbulator (m)
e/h	Relative height of semicircular turbulator (-)
p/e	Relative pitch of turbulator (-)
$\dot{m}$	Mass flow rate (kg/s)
Greek symbols	
η	Efficiency (%)
α	Increase ratio of semicircular turbulator (-)
Subscripts	
in	Inlet
out	Outlet
pv	Photovoltaic module
pvtc	Photovoltaic thermal collector
th	Thermal
e	Electrical
o	Overall

References

1. Piliougine, M.; Oukaja, A.; Sidrach-de-Cardona, M.; Spagnuolo, G. Temperature Coefficients of Degraded Crystalline Silicon Photovoltaic Modules at Outdoor Conditions. *Prog. Photovolt. Res. Appl.* **2021**, *29*, 558–570. [CrossRef]
2. Cui, Y.; Zhu, J.; Zhang, F.; Shao, Y.; Xue, Y. Current Status and Future Development of Hybrid PV/T System with PCM Module: 4E (Energy, Exergy, Economic and Environmental) Assessments. *Renew. Sustain. Energy Rev.* **2022**, *158*, 112147. [CrossRef]
3. Wolf, M. Performance Analyses of Combined Heating and Photovoltaic Power Systems for Residences. *Energy Convers. Manag.* **1976**, *16*, 79–90. [CrossRef]
4. Yadav, A.S.; Bhagoria, J.L. A CFD Based Thermo-Hydraulic Performance Analysis of an Artificially Roughened Solar Air Heater Having Equilateral Triangular Sectioned Rib Roughness on the Absorber Plate. *Int. J. Heat Mass Transf.* **2014**, *70*, 1016–1039. [CrossRef]
5. Yadav, A.S.; Bhagoria, J.L. A Numerical Investigation of Square Sectioned Transverse Rib Roughened Solar Air Heater. *Int. J. Therm. Sci.* **2014**, *79*, 111–131. [CrossRef]
6. Kumar, A.; Kim, M.-H. Thermal Hydraulic Performance in a Solar Air Heater Channel with Multi V-Type Perforated Baffles. *Energies* **2016**, *9*, 564. [CrossRef]
7. Kumar, R.; Goel, V.; Kumar, A. Investigation of Heat Transfer Augmentation and Friction Factor in Triangular Duct Solar Air Heater Due to Forward Facing Chamfered Rectangular Ribs: A CFD Based Analysis. *Renew. Energy* **2018**, *115*, 824–835. [CrossRef]

8. Kim, S.; Kim, J.; An, B.; Kim, Y.; Son, C.; Yoon, J.; Choi, K. Heat Transfer Performance and Pressure Drop Analysis According to Shape Conditions of Turbulent Promoters and Flow Conditions in Air-Type PV/T Collectors. *J. Korean Sol. Energy Soc.* **2022**, *42*, 87–101. [CrossRef]
9. Kim, J.; Kim, S.; An, B.; Choi, H.; Choi, K. Evaluation of Heat Transfer Performance Depending on Semicircular Turbulence Promoter Shape Conditions and Flow Conditions in the Air-Type PV/T Collector. *J. Korean Sol. Energy Soc.* **2022**, *42*, 47–61. [CrossRef]
10. Jha, P.; Das, B.; Gupta, R. An Experimental Study of a Photovoltaic Thermal Air Collector (PVTAC): A Comparison of a Flat and the Wavy Collector. *Appl. Therm. Eng.* **2019**, *163*, 114344. [CrossRef]
11. Kabeel, A.E.; Hamed, M.H.; Omara, Z.M.; Kandeal, A.W. Solar Air Heaters: Design Configurations, Improvement Methods and Applications—A Detailed Review. *Renew. Sustain. Energy Rev.* **2017**, *70*, 1189–1206. [CrossRef]
12. Varun Kumar, B.; Manikandan, G.; Rajesh Kanna, P.; Taler, D.; Taler, J.; Nowak-Ocłón, M.; Mzyk, K.; Toh, H.T. A Performance Evaluation of a Solar Air Heater Using Different Shaped Ribs Mounted on the Absorber Plate—A Review. *Energies* **2018**, *11*, 3104. [CrossRef]
13. Singh, V.P.; Jain, S.; Karn, A.; Kumar, A.; Dwivedi, G.; Meena, C.S.; Dutt, N.; Ghosh, A. Recent Developments and Advancements in Solar Air Heaters: A Detailed Review. *Sustainability* **2022**, *14*, 12149. [CrossRef]
14. Sopian, K.; Yigit, K.S.; Liu, H.T.; Kakaç, S.; Veziroglu, T.N. Performance Analysis of Photovoltaic Thermal Air Heaters. *Energy Convers. Manag.* **1996**, *37*, 1657–1670. [CrossRef]
15. Raman, V.; Centre, G.N.T. A Comparison Study of Energy and Exergy Performance of a Hybrid Photovoltaic Double-Pass and Single-Pass Air Collector. *Int. J. Energy Res.* **2009**, *33*, 605–617. [CrossRef]
16. Kumar, R.; Rosen, M.A. Performance Evaluation of a Double Pass PV/T Solar Air Heater with and without Fins. *Appl. Therm. Eng.* **2011**, *31*, 1402–1410. [CrossRef]
17. Amori, K.E.; Abd-AlRaheem, M.A. Field Study of Various Air Based Photovoltaic/Thermal Hybrid Solar Collectors. *Renew. Energy* **2014**, *63*, 402–414. [CrossRef]
18. Hegazy, A.A. Comparative Study of the Performances of Four Photovoltaic/Thermal Solar Air Collectors. *Energy Convers. Manag.* **2000**, *41*, 861–881. [CrossRef]
19. Hussain, F.; Othman, M.Y.H.; Sopian, K.; Yatim, B.; Ruslan, H.; Othman, H. Design Development and Performance Evaluation of Photovoltaic/Thermal (PV/T) Air Base Solar Collector. *Renew. Sustain. Energy Rev.* **2013**, *25*, 431–441. [CrossRef]
20. Ooshaksaraei, P.; Sopian, K.; Zaidi, S.H.; Zulkifli, R. Performance of Four Air-Based Photovoltaic Thermal Collectors Configurations with Bifacial Solar Cells. *Renew. Energy* **2017**, *102*, 279–293. [CrossRef]
21. Chaibi, Y.; El Rhafiki, T.; Simón-Allué, R.; Guedea, I.; Luaces, S.C.; Gajate, O.C.; Kousksou, T.; Zeraouli, Y. Air-Based Hybrid Photovoltaic/Thermal Systems: A Review. *J. Clean. Prod.* **2021**, *295*, 126211. [CrossRef]
22. Othman, M.Y.; Yatim, B.; Sopian, K.; Abu Bakar, M.N. Performance Studies on a Finned Double-Pass Photovoltaic-Thermal (PV/T) Solar Collector. *Desalination* **2007**, *209*, 43–49. [CrossRef]
23. Choi, H.U.; Choi, K.H. Performance Evaluation of PV/T Air Collector Having a Single-Pass Double-Flow Air Channel and Non-Uniform Cross-Section Transverse Rib. *Energies* **2020**, *13*, 2203. [CrossRef]
24. Alam, T.; Meena, C.S.; Balam, N.B.; Kumar, A.; Cozzolino, R. Thermo-Hydraulic Performance Characteristics and Optimization of Protrusion Rib Roughness in Solar Air Heater. *Energies* **2021**, *14*, 3159. [CrossRef]
25. Zhang, J.; Diao, Y.H.; Zhao, Y.H.; Zhang, Y.N. An Experimental Study of the Characteristics of Fluid Flow and Heat Transfer in the Multiport Microchannel Flat Tube. *Appl. Therm. Eng.* **2014**, *65*, 209–218. [CrossRef]